IEEE Access
Multidisciplinary | Rapid Review | Open Access Journal

Received September 17, 2019, accepted October 7, 2019, date of publication October 11, 2019, date of current version October 23, 2019.

Digital Object Identifier 10.1109/ACCESS.2019.2946719

~3.5 μm Er^{3+}: ZBLAN Fiber Laser in Dual-End Pumping Regime

CHUNXIANG ZHANG[1], JIADONG WU[1], PINGHUA TANG[2], CHUJUN ZHAO[1], AND SHUANGCHUN WEN[1]

[1]Key Laboratory for Micro/Nano Optoelectronic Devices of Ministry of Education and Hunan Provincial Key Laboratory of Low-Dimensional Structural Physics and Devices, School of Physics and Electronics, Hunan University, Changsha 410082, China
[2]School of Physics and Optoelectronics, Xiangtan University, Xiangtan 411105, China

Corresponding author: Pinghua Tang (pinghuatang@xtu.edu.cn)

This work was supported in part by the National Natural Science Foundation of China under Grant 61605166, Grant 61875132, and Grant 61805115, in part by the China Postdoctoral Science Foundation under Grant 2017M620349, and in part by the Natural Science Foundation of Hunan Province under Grant 2018JJ3514.

ABSTRACT Mid-infrared (mid-IR) fiber laser sources at 3.5 μm have wide applications in spectroscopy, environmental monitoring, medicine, and defense countermeasures. In this work, we experimentally investigate a dual-end double wavelength pumped (i.e. both fiber ends pumped by 976 nm and 1973 nm, respectively) Er^{3+}: ZBLAN fiber laser at 3.5 μm in detail. In the experiment, we carefully evaluate the lasing characteristics in terms of output power and scalability in contrast to the single-end pumping regime. The dual-end pumped Er^{3+}: ZBLAN fiber laser yields a maximum output power of 1.72 W at the launched 1973 nm pump power of 8.39 W limited only by the available output power of the 1973 nm laser pump. The operation wavelength is experimentally found to be in a range from 3440 nm to 3620 nm depending on the pump power level. Lasing characteristics for Er^{3+}: ZBLAN fibers with different lengths and doping concentrations and other cavity parameters are also investigated in this pumping regime to optimize the lasing performance.

INDEX TERMS Fiber optics oscillator, erbium, mid-infrared laser.

I. INTRODUCTION

Mid-infrared (mid-IR) fiber laser sources emitting near 3 μm have attracted considerable attention in recent years based on the significant progress in the fabrication of rare-earth-doped fluoride gain fibers including Erbium (Er^{3+}) [1], [2], Holmium (Ho^{3+}) [3], Dysprosium (Dy^{3+}) [4], [5], as well as, the development of relative mid-IR passive components such as dichroic mirror, fiber Bragg grating (FBG) and saturable absorber. Particularly, laser radiations in the specific 3.5 μm spectral region can have numerous practical and scientific applications in spectroscopy, environmental monitoring, medicine, defense countermeasures and many others [6]–[8], because this region corresponds to the transparency window of the atmosphere and strong absorption peaks of many molecules containing covalent bonds between carbon and hydrogen, or nitrogen or oxygen (such as CH_4, HCN, CO_2, CO) [9]–[12]. Typical approaches to generating the 3.5 μm laser emissions are usually based on optical parametric oscillators (OPOs) [13], [14], quantum cascade lasers (QCLs) [15], Raman fiber lasers (RFLs) [16], [17], and rare-earth-doped fluoride fiber lasers [18]–[22]. Indirect nonlinear frequency down-conversion techniques like OPOs and RFLs can allow for flexibility in the operating wavelength and can easily extend to the mid-IR wavelength region. However, they suffer from disadvantages like low efficiency, high complexity, and high cost. Although QCLs can produce laser emissions at 3.5 μm directly, the output powers are normally limited to below the level of hundreds of milliwatts at room temperature [15]. In contrast, rare-earth-doped fiber lasers benefitting from high efficiency, long-term stability, compactness, excellent beam quality, and high-power scalability can show better prospects in future applications.

Early on, H. Többen et al. realized the 3.5 μm laser emission from an Er^{3+}-doped fluoride glass gain medium at room temperature pumped by a dicyanomethylene (DCM) dye laser at 655 nm [23]. In this visible light pumping scheme, the Er^{3+}-doped fluoride glass laser yielded an output power of

The associate editor coordinating the review of this manuscript and approving it for publication was Zinan Wang.

only 10 mW with a very low slope efficiency of 2.8% due to the large quantum defect. O. Henderson-Sapir et al. recently proposed a dual-wavelength pumping (DWP) scheme in Er^{3+}-doped ZBLAN fluoride (Er^{3+}: ZBLAN) fiber lasers, where simultaneous pumping with ~976 nm and ~1973 nm lasers are used to achieve the 3.5 μm mid-IR laser effectively [18]. They used this DWP technique to obtain an output power of 260 mW with a slope efficiency of ~25% with respect to the 1973 nm pump power in a laser cavity based on bulk reflectors. With further cavity configuration optimization, such as introducing FBGs or diffraction gratings as the cavity reflector and wavelength-selection component, the output power was increased to the watt level in the 3.5 μm wavelength region [19], [20]. All these configurations employed a single-end pumping regime for the two pump lasers in mid-IR Er^{3+}: ZBLAN fluoride fiber lasers. Such a pumping configuration can expose the fluoride gain fiber tip at the pump injection side to a significant thermal loading density due to both the high launched pump powers and intense intra-cavity laser power density, which can possibly induce its thermal damage because of the lower damage threshold compared to its silica counterparts. In addition, the related thermal effects caused by the large quantum defect between the pump wavelength and the laser wavelength can increase the multiphoton relaxation rate in the high-power operation regime. These factors greatly limit the further power scaling capability and stability of the 3.5 μm Er^{3+}-doped fluoride fibers.

F. Maes et al. used a monolithic cavity design comprising of a pair of FBGs written in the fluoride gain fiber to avoid the exposure to the intense intra-cavity laser light for both fiber tips, and thus relieve the thermal load accumulated in both fiber end facets [21]. They achieved a record output power of 5.6 W at 3.5 μm. Later on, they employed a dual-end pumping regime in a heavily-erbium-doped fluoride fiber laser (erbium doping concentration of 7 mol.%), and realized 3.4 W laser emission at 3.5 μm [24]. Almost at the same time, H. Y. Luo et al. also reported a watt-level gain-switched fiber laser at 3.5 μm based on a dual-end pumping scheme [25]. It is worth noting that, the dual-end pumping regime, where the 976 nm and 1973 nm pump lasers are respectively launched into both opposite fiber ends to pump the gain fiber, can be used to alleviate the thermal load in the fiber tips at the pump launch sides, providing an approach to further improving the laser power scalability. At the same time, in this dual-end pumping regime, both pump laser beams can be aligned and launched independently, which reduces the complexity of adjustment and maintenance and guarantees high operation stability.

In this work, we demonstrate a high-power dual-end pumped Er^{3+}: ZBLAN fiber laser at 3.5 μm and carefully investigate the lasing characteristics in terms of output power and scalability in the dual-end pumping regime. The dual-end pumped Er^{3+}: ZBLAN fiber laser yields a maximum output power of 1.72 W at the launched 1973 nm pump power of 8.39 W limited only by the available output power

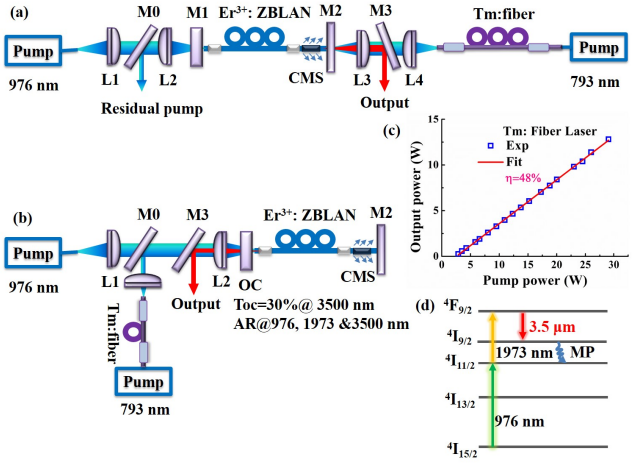

FIGURE 1. (a) and (b) Experimental schematic diagrams of the dual-end and single-end pumped 3.5μm Er^{3+}: ZBLAN fiber laser; (c) the laser input-output power relationship of the 1973 nm Tm-doped fiber laser pump; (d) the simplified energy diagram of the Er^{3+} ion involved. MP, multi-phonon.

of the 1973 nm laser pump. Lasing characteristics for Er^{3+}: ZBLAN fibers with different lengths and doping concentrations and other cavity parameters are also investigated in this pumping regime to optimize the lasing performance.

II. EXPERIMENTAL SETUP

The experimental schematic diagram of the 3.5 μm dual-end pumped Er^{3+}: ZBLAN fiber laser is presented in Fig. 1(a). The pump lasers employed in our experiment are a commercially available 976 nm fiber-coupled laser diode (Shenzhen MChlight Company Ltd) and an in-house built Tm-doped single-mode silica fiber laser operating at 1973 nm. The 20 W 976 nm laser diode has a pigtail fiber with a core diameter of 105 μm and a numerical aperture (NA) of 0.22, the laser beam of which was collimated (by L1, N-BK7, coating-B, f=25.4 mm) and focused (by L2, N-BK7, coating-C, f=25.4 mm) onto one fiber end facet with a measured coupling efficiency of 90% in the regime of cladding-pumping. The output beam from another 1973 nm fiber laser pump with a maximum output power of 12.8 W (shown in Fig. 1(c)) was collimated and focused into the core of the opposite fiber end in the core pumping regime by a pair of broadband antireflection-coated ZnSe aspheric lenses L4 (f = 25.4 mm) and L3 (f = 25.4 mm), respectively, through careful alignment.

The gain fibers used in the experiment are purchased from FiberLabs in Japan: the first is a 2 m double-clad Er^{3+}: ZBLAN fiber with an Er^{3+} dopant concentration of 1.5 mol.% that has a 20 μm core with a numerical aperture (NA) of 0.2 and a 250 μm circular inner cladding with a NA of 0.5 surrounded by a low index polymer jacket as the outer cladding; the second one is a 5 m double-clad Er^{3+}: ZBLAN fiber with an Er^{3+} dopant concentration of 1 mol.% that has a 16 μm core with a NA of 0.2 and a 250 μm circular inner cladding with a NA of 0.5.

The lasing feedback is provided by a simple optical arrangement employing two dielectric mirrors: one is a dichroic mirror M1 that is highly reflective at the lasing wavelength of 3.5 μm and transmissive at both pump wavelengths of 976 nm and 1973 nm, and the other dichroic mirror M2 has a high reflectivity at 976 nm and a high transmission at 1973 nm. Besides, M2 act as the output coupler (OC) with a transmission of 30% or 65% at the 3.5 μm band. Both fiber end facets were perpendicularly cleaved by a liquid clamp cleaver (3SAE II LDF, USA) to offer a perfect butted joint against the two-cavity mirrors, and then were carefully mounted in fan-cooled V-groove heat sinks to prevent possible thermal damage to the fiber coatings. In addition, a cladding-mode stripper (CMS) comprising of a high refractive index matching liquid (Cargille Labs Inc.) was also implemented to simultaneously remove most of the 1973 nm pump light coupling into the fiber cladding and the residual 976 nm pump power to greatly protect the pump injection end and to operate the core-launch alignment easily. Another dichroic mirror M3 with high reflectivity at the 3.5 μm lasing wavelength and high transmission at the 1973 nm pump wavelength was positioned at 45° in the 1973 nm pump path to extract the laser output. The residual 1973 nm pump beam was extracted out by the dichroic mirror M0 that has a high reflectivity at the 1973 nm pump wavelength and high transmission at the 976 nm pump wavelength.

The output spectrum was measured using a Fourier Transform Optical Spectrum Analyzer with a FC/PC fluoride fiber-coupled input port (OSA207C, Thorlabs, USA) with a nominal resolution of ~0.2 nm at ~3 μm wavelength band. A real-time oscilloscope with a bandwidth of 4 GHz (Agilent Technol., DSO9404A), together with a HgCdTe detector (VIGO System, PCI-9, <~2 ns rise-time at 1-9 μm) were simultaneously used to monitor the short-term stability of the laser output.

III. RESULTS AND DISCUSSIONS

Firstly, the residual pump absorption characteristics without lasing feedback (cavity mirrors tilted) and the CMS are evaluated for the two types of gain fibers with different doping concentrations to estimate the core-launch efficiency: one is 2 m 1.5 mol.% Er^{3+}: ZBLAN fiber and the other one is 2.85 m 1 mol.% Er^{3+}: ZBLAN fiber, as shown in Fig. 2(a) and 2(b), respectively. Figure 2 shows that, for both fibers, the residual 1973 nm pump powers decrease remarkably with the launched 976 nm pump power under different launched 1973 nm pump levels, which is attributed to the increasingly accumulated ions on the ''virtual'' ground state of level $^4I_{11/2}$ when the 976 nm pump power is increased. However, only those pump light launched into the fiber core can be effectively depleted with enough 976 nm pump power. Therefore, from the residual 1973 nm pump powers from two gain fibers, when adequate 976 nm pump power is provided, we can estimate the fiber core launch efficiency of the 1973 nm pump light to be 70 % and 67 % for the 1.5 mol.% Er^{3+}: ZBLAN and 1 mol.% Er^{3+}: ZBLAN fibers, respectively. It is also worth noting that when the lasing feedback is formed, the launched 976 nm pump power required to deplete the 1973 nm pump light would be significantly lower than it would without cavity feedback.

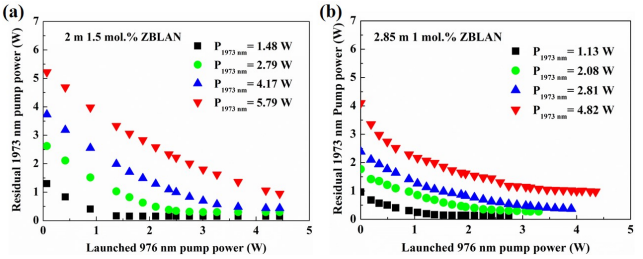

FIGURE 2. Residual pump powers of 1973 nm versus launched pump power of 976 nm under different launched 1973 nm pump powers for two different gain fibers without lasing feedback: (a) 2 m 1.5 mol.% Er^{3+}: ZBLAN fiber; (b) 2.85 m 1 mol.% Er^{3+}: ZBLAN fiber.

We started testing the lasing characteristics of the 2 m 1.5 mol.% Er^{3+}: ZBLAN fiber first by employing an output coupler with a transmission of 30%. The 2.8 μm laser emission was observed when only a 976 nm pump beam was launched, which could be easily suppressed and eliminated when the second 1973 nm pump was introduced. Figure 3(a) depicts the average output powers as a function of the launched pump power of 1973 nm under different launched 976 nm pump powers. For P_{976} nm=1.61 W there is a significant decrease of output power when the 1973 nm pump power goes beyond 3.2 W. The output power rollover can be attributed to the laser quenching effect that results from the non-resonant excited state absorption (ESA) of 1973 nm, which depletes ions on the upper laser level of the 3.5 μm transition and leads to the lack of ions in the virtual ground state ($^4I_{11/2}$ level) [24]. By increasing the launched 976 nm pump power, the 1973 nm pump power at which the output power begins to be quenched also increases. When the launched 976 nm pump power is beyond 3.64 W, the output power is almost linearly dependent on the 1973 nm pump power. The obtained maximum output power from the laser is 1.21 W at the launched 1973 nm pump power of 5.34 W with an initial slope efficiency of up to 33.6%. Further increasing the 1973 nm launched pump power resulted in no significant output power rise. The lasing efficiency decreased slightly when the launched 1973 nm pump power exceeded 3.5 W. In this pump range the free-running operation wavelength is redshifted.

Figure 4 displays the measured corresponding output spectra. When the launched 1973 nm pump power is lower than 3.5 W, the fiber laser operated in 3442 nm with a corresponding full width at half-maximum (FWHM) bandwidth of about 0.7 nm. Above this pump power, the operating wavelength switched to 3533 nm and the bandwidth increased slightly, to about 0.8 nm. This sudden shift might be attributed to the following reason. In the high power operation, the populations of the lower laser sublevel of $^4I_{9/2}$ are too excessive to

empty fast enough, which leads to longer-wavelength lasing by transiting to a higher sublevel of $^4I_{9/2}$ [22].

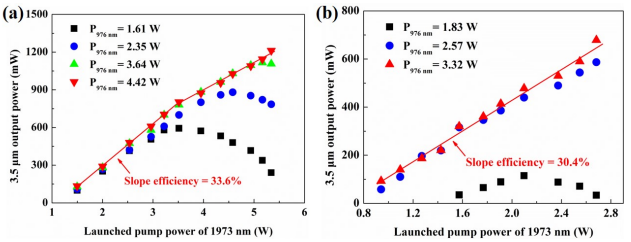

FIGURE 3. Output powers of the ~3.5μm Er^{3+}-doped fluoride fiber laser with respect to the launched 1973 nm pump power under: (a) the dual-end pumping regime for $P_{976\,nm}$ = 1.61, 2.35, 3.64, and 4.42 W, respectively; (b) the single-end pumping regime for $P_{976\,nm}$ = 1.83, 2.57, and 3.32 W, respectively.

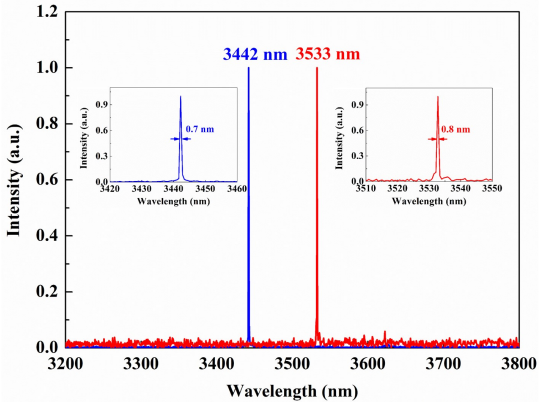

FIGURE 4. Output spectra of the dual-end pumped Er^{3+}-doped fluoride fiber laser with a 2 m 1.5 mol.% Er^{3+}: ZBLAN gain fiber.

For comparison, we also performed the single-end pumping scheme using a similar experiment configuration depicted in Ref. [22], as is shown in Fig. 1(d). However, in this single-end pumped Er^{3+}: ZBLAN fiber laser, the operation stability can be greatly deteriorated when the launched 1973 nm pump power reaches over 4.5 W. To guarantee excellent operation stability without fiber tip damage, we measured and recorded the output powers at different launched 1973 nm pump power extending to near 3 W, as shown in Fig. 3(b). The maximum average output power is 679 mW at 2.68 W launched 1973 nm pump power with a corresponding slope efficiency of 30.4%. Any further large increase in the launched pump power of 1973 nm will result in frequently operating wavelength redshifting and a great possibility of fiber tip damage. Despite these existing issues, the threshold pump power of single-end pumping scheme is lower than in the dual-end pumping one since the 1973nm light does not need to travel the full length of the fiber to be absorbed.

A comparative study was also conducted to evaluate the lasing performance of a lightly doped 1 mol.% Er^{3+}: ZBLAN fiber with output couplers of 30 and 65% transmission (Toc). To guarantee the efficient pump absorption we employed a fiber length of 5 m. The output powers as a function of the launched 1973 nm pump power are shown in Fig. 5. We can see that the laser can also have the quenching effect beginning at 2.8 W launched 1973 nm pump power under the case with insufficient 976 nm pump power of 0.81 W. The laser decrease behavior disappears with increasing the launched 976 nm pump power to 1.53 W and above. For these launched 976 nm pump powers, the lasing performance exhibits almost the same in terms of laser threshold and slope efficiency for either Toc=30% or 65%, which indicates that the number of active ions staying on the virtual ground state is sufficient to be excited to upper laser level under the current 1973 nm pump levels. In contrast to the linear dependence of laser power on the launched 1973 nm pump power for Toc=65%, under Toc=30% the laser output power curve exhibits some obvious rollovers which are not arising from the quenching effect induced by insufficient 976 nm pump power. Instead, we can attribute this to the change of gain since in this situation the operation wavelength is significantly redshifted, spanning several tens of nanometers at these certain launched pump powers, like 3.62 W and 5.73 W.

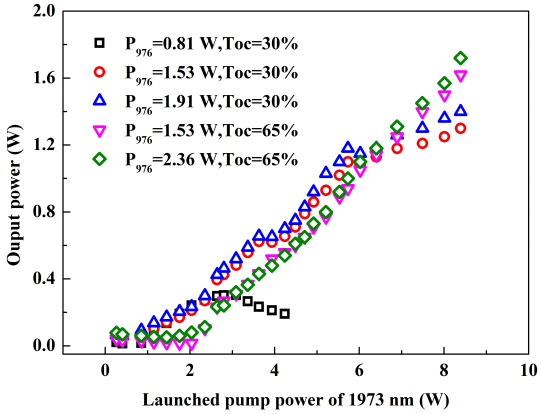

FIGURE 5. Output powers as a function of launched 1973 nm pump power of the dual-end pumped Er $^{3+}$-doped fluoride fiber laser with a 5 m 1 mol.% Er^{3+}: ZBLAN gain fiber.

In other 1973 nm pump power range, the operation wavelength progresses slightly from the short-wavelength side of 3440 nm to the long-wavelength side of 3620 nm when the pump power increases from 1.14 to 8.39 W, corresponding to an overall range of as much as 180 nm. The output spectra at different 1973 nm pump power levels are typically shown in Fig. 6. At some specific pump powers in the middle pump range and above, the laser output spectrum can feature multiple peaks where the power distribution tends to shift to long-wavelength lines when the pump power increases. In the 3.5 μm Er^{3+}: ZBLAN fiber laser system with a smaller transmission (Toc=30%), the lower overall cavity loss results in a small lasing threshold for all possible laser emissions that come from the transitions between specific Stark sublevels of the upper and lower laser levels. They can compete during the whole pump increasing process and only those laser lines with equivalent gains can ultimately survive. By contrast, for Toc=65% the operation wavelength is fixed at 3440 nm and a maximum output power of 1.72 W is obtained at the launched

1973 nm pump power of 8.39 W, limited only by the available 1973 nm pump power. The larger output coupler transmission in the laser cavity makes it possible for only the laser wavelength with the largest gain to survive during the whole pump power range, which makes the output wavelength relatively pure.

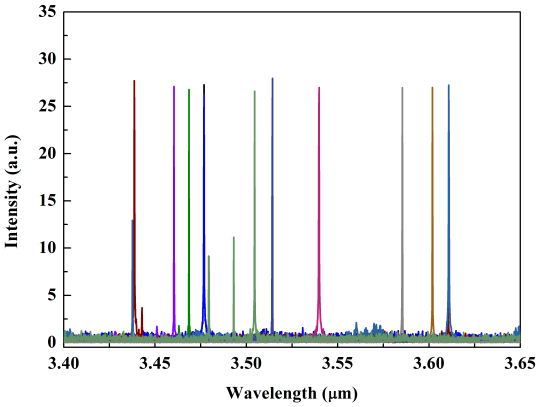

FIGURE 6. Output spectra of the dual-end pumped Er^{3+}-doped fluoride fiber laser (Toc=30%) with a 5 m 1 mol.% Er^{3+}: ZBLAN gain fiber at different 1973 nm pump power levels.

Concerning the Er^{3+} doping concentrations in Er^{3+}: ZBLAN gain fibers, a low Er^{3+} doping concentration is believed to be preferable for efficient laser operation since high Er^{3+}-doping not only leads to an increased threshold pump power but also a significant degradation in laser performance due to nonnegligible interionic energy transfer processes like energy-transfer-upconversion (ETU) and cross-relaxation effects that will lead to the accumulation of ions in the lower laser level and the escape of ions from the upper laser level. These interactions occur between active ions and their strengths are directly dependent on the doping concentration [26], [27]. Besides, to guarantee more efficient absorption of the pump light, a longer gain fiber length is usually used for gain fibers with a low doping concentration, which can enable the yielded heat load distributed uniformly across the fiber and allow for further power scalability. Higher lasing efficiencies should be achievable with gain fibers of improved quality, as well as reasonable doping concentration minimizing the effects of ETU and cross-relaxation processes and optimized resonator design (such as optimizing the transmission of output couplers).

To test the long-term power stability of the dual-end pumped Er^{3+}: ZBLAN fiber laser, the corresponding output power at the launched 1973 nm pump power of 6.89 W was monitored for 10 minutes, as shown in Fig. 7. The RMS output power fluctuation is about 0.48% and the peak-to-peak power deviation is 2.32%. The slight power fluctuations can be attributed to the mechanical vibrations of the pump source and fiber end facets, which will change the coupling efficiency of the 1973 nm pump beam to the fiber core. In addition, mechanical vibrations of the bulk reflectors can also influence the power stability of the fiber laser since they connect directly with the intra-cavity lasing feedback. Future substituting the bulk reflectors with FBGs will guarantee an improved laser power scaling capability and stability.

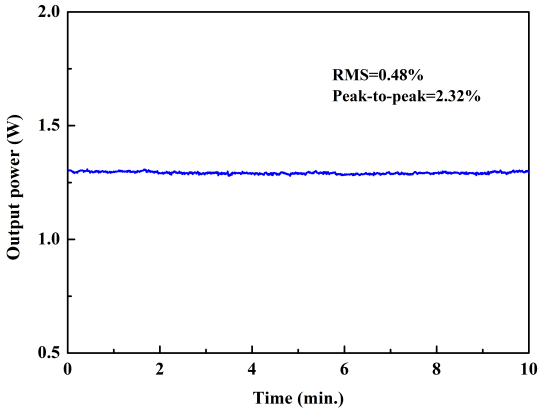

FIGURE 7. Power stability of the dual-end pumped Er^{3+}-doped fluoride fiber laser.

IV. CONCLUSION

A dual-end double wavelength pumping scheme in the 3.5 μm Er^{3+}-doped fluoride fiber laser is investigated in detail. Lasing characteristics for gain fibers with different lengths and doping concentrations and other cavity parameters like transmissions of the output coupler to improve the lasing performance are investigated. We demonstrate that, to some extent, this pumping regime can prevent the fiber tip damage in moderate pump power levels, in contrast to the single-end pumping scheme, and therefore allows for further power scalability. A maximum output power of 1.72 W is obtained at the launched 1973 nm pump power of 8.39 W limited only by the available output power of the 1973 nm laser pump.

REFERENCES

[1] V. Fortin, M. Bernier, S. T. Bah, and R. Vallée, "30 W fluoride glass all-fiber laser at 2.94 μm," *Opt. Lett.*, vol. 40, no. 12, pp. 2882–2885, Jun. 2015.
[2] P. Tang, Z. Qin, J. Liu, C. Zhao, G. Xie, S. Wen, and L. Qian, "Watt-level passively mode-locked Er^{3+}-doped ZBLAN fiber laser at 2.8 μm," *Opt. Lett.*, vol. 40, no. 21, pp. 4855–4858, Nov. 2015.
[3] F. Maes, V. Fortin, S. Poulain, M. Poulain, J. Carrée, M. Bernier, and R. Vallée, "Room-temperature fiber laser at 3.92 μm," *Optica*, vol. 5, no. 7, pp. 761–764, Jun. 2018.
[4] R. I. Woodward, M. R. Majewski, G. Bharathan, D. D. Hudson, A. Fuerbach, and S. D. Jackson, "Watt-level dysprosium fiber laser at 3.15 μm with 73% slope efficiency," *Opt. Lett.*, vol. 43, no. 7, pp. 1471–1474, Mar. 2018.
[5] L. Sójka, L. Pajewski, M. Popenda, E. Beres-Pawlik, S. Lamrini, K. Markowski, T. Osuch, T. M. Benson, A. B. Seddon, and S. Sujecki, "Experimental investigation of mid-infrared laser action from Dy^{3+} doped fluorozirconate fiber," *IEEE Photon. Technol. Lett.*, vol. 30, no. 12, pp. 1083–1086, Jun. 15, 2018.
[6] S. D. Jackson, "Towards high-power mid-infrared emission from a fibre laser," *Nature Photon.*, vol. 6, no. 6, pp. 423–431, Jun. 2012.
[7] V. Fortin, M. Bernier, N. Caron, D. Faucher, M. El-Amraoui, Y. Messaddeq, and R. Vallée, "Towards the development of fiber lasers for the 2 to 4 μm spectral region," *Opt. Eng.*, vol. 52, no. 5, May 2013, Art. no. 054202.

[8] O. Henderson-Sapir, A. Malouf, N. Bawden, J. Munch, S. D. Jackson, and D. J. Ottaway, "Recent advances in 3.5 μm erbium-doped mid-infrared fiber lasers," *IEEE J. Sel. Topics Quantum Electron.*, vol. 23, no. 3, May/Jun. 2017, Art. no. 0900509.
[9] A. Schliesser, N. Picqué, and T. W. Hänsch, "Mid-infrared frequency combs," *Nature Photon.*, vol. 6, no. 7, pp. 440–449, Jul. 2012.
[10] B. Molocher, "Countermeasure laser development," *Proc. SPIE*, vol. 5989, Nov. 2005, Art. no. 598902.
[11] B. M. Walsh, H. R. Lee, and N. P. Barnes, "Mid infrared lasers for remote sensing applications," *J. Lumin.*, vol. 169, pp. 400–405, Jan. 2016.
[12] S.-S. Kim, C. Young, B. Vidakovic, S. G. A. Gabram-Mendola, C. W. Bayer, and B. Mizaikoff, "Potential and challenges for mid-infrared sensors in breath diagnostics," *IEEE Sensors J.*, vol. 10, no. 1, pp. 145–158, Jan. 2010.
[13] M. Ebrahim-Zadeh and S. C. Kumar, "Yb-fiber-laser-pumped ultrafast frequency conversion sources from the mid-infrared to the ultraviolet," *IEEE J. Sel. Topics Quantum Electron.*, vol. 20, no. 5, Sep./Oct. 2014, Art. no. 7600519.
[14] Y. Shang, M. Shen, P. Wang, X. Li, and X. Xu, "Amplified random fiber laser-pumped mid-infrared optical parametric oscillator," *Chin. Opt. Lett.*, vol. 14, no. 12, Dec. 2016, Art. no. 121901.
[15] M. Razeghi, N. Bandyopadhyay, Y. Bai, Q. Lu, and S. Slivken, "Recent advances in mid infrared (3-5μm) quantum cascade lasers," *Opt. Mater. Express*, vol. 3, no. 11, pp. 1872–1884, Oct. 2013.
[16] M. Bernier, V. Fortin, N. Caron, M. Ei-Amraoui, Y. Messaddeq, and R. Vallée, "Mid-infrared chalcogenide glass Raman fiber laser," *Opt. Lett.*, vol. 38, no. 2, pp. 127–129, Jan. 2013.
[17] M. Bernier, V. Fortin, M. El-Amraoui, Y. Messaddeq, and R. Vallée, "3.77 μm fiber laser based on cascaded Raman gain in a chalcogenide glass fiber," *Opt. Lett.*, vol. 39, no. 7, pp. 2052–2055, Apr. 2014.
[18] O. Henderson-Sapir, J. Munch, and D. J. Ottaway, "Mid-infrared fiber lasers at and beyond 3.5 μm using dual-wavelength pumping," *Opt. Lett.*, vol. 39, no. 3, pp. 493–496, Feb. 2014.
[19] V. Fortin, F. Maes, M. Bernier, S. T. Bah, M. D'Auteuil, and R. Vallée, "Watt-level erbium-doped all-fiber laser at 3.44 μm," *Opt. Lett.*, vol. 41, no. 3, pp. 559–562, Jan. 2016.
[20] O. Henderson-Sapir, S. D. Jackson, and D. J. Ottaway, "Versatile and widely tunable mid-infrared erbium doped ZBLAN fiber laser," *Opt. Lett.*, vol. 41, no. 7, pp. 1676–1679, 2016.
[21] F. Maes, V. Fortin, M. Bernier, and R. Vallée, "5.6 W monolithic fiber laser at 3.55 μm," *Opt. Lett.*, vol. 42, no. 11, pp. 2054–2057, May 2017.
[22] Z. Qin, G. Xie, J. Ma, P. Yuan, and L. Qian, "Mid-infrared Er: ZBLAN fiber laser reaching 3.68 μm wavelength," *Chin. Opt. Lett.*, vol. 15, no. 11, Nov. 2017, Art. no. 111402.
[23] H. Többen, "Room temperature CW fibre laser at 3.5 μm in Er^{3+}-doped ZBLAN glass," *Electron. Lett.*, vol. 28, no. 14, pp. 1361–1362, Jul. 1992.
[24] F. Maes, C. Stihler, L.-P. Pleau, V. Fortin, J. Limpert, M. Bernier, and R. Vallée, "3.42 μm lasing in heavily-erbium-doped fluoride fibers," *Opt. Express*, vol. 27, no. 3, pp. 2170–2183, Feb. 2019.
[25] H. Luo, J. Yang, F. Liu, Z. Hu, Y. Xu, F. Yan, H. Peng, F. Ouellette, J. Li, and Y. Liu, "Watt-level gain-switched fiber laser at 3.46 μm," *Opt. Express*, vol. 27, no. 2, pp. 1367–1375, Jan. 2019.
[26] F. Maes, V. Fortin, M. Bernier, and R. Vallée, "Quenching of 3.4 μm dual-wavelength pumped erbium doped fiber lasers," *IEEE J. Quantum Electron.*, vol. 53, no. 2, Apr. 2017, Art. no. 1600208.
[27] M. Gorjan, M. Marincek, and M. Copic, "Role of interionic processes in the efficiency and operation of erbium-doped fluoride fiber lasers," *IEEE J. Quantum Electron.*, vol. 47, no. 2, pp. 262–273, Feb. 2011.

CHUNXIANG ZHANG is currently pursuing the Ph.D. degree with the School of Physics and Electronics, Hunan University, Changsha, China. Her research interests include fiber lasers and nonlinear optics.

JIADONG WU is currently pursuing the Ph.D. degree with the School of Physics and Electronics, Hunan University, Changsha, China. His research interest includes fiber lasers.

PINGHUA TANG received the Ph.D. degree from the School of Physics and Electronics, Hunan University, Changsha, China, in 2015. He is currently an Associate Professor with Xiangtan University, Xiangtan, China. He has authored or coauthored more than 30 journal articles. His current research interests include fiber lasers, solid-state lasers, and nonlinear optics.

CHUJUN ZHAO received the Ph.D. degree in optics from the Shanghai Institute of Optics and Fine Mechanics, Chinese Academy of Sciences, Shanghai, China, in 2008. He is currently a Professor with Hunan University, Changsha, China. His current research interests include fiber lasers, solid-state lasers, and nonlinear optics.

SHUANGCHUN WEN received the Ph.D. degree in optics from the Shanghai Institute of Optics and Fine Mechanics, Chinese Academy of Sciences, Shanghai, China, in 2001. He is currently a Professor with Hunan University, Changsha, China. His current research interests include photonic materials and devices, solid-state/fiber lasers, and nonlinear optics. He is a member of the Optical Society of America and the International Society for Optical Engineering.